Supporting Information: High-refractive-index 2D photonic structures for robust low-threshold multiband lasing

Ana Conde-Rubio,† Juan R. Deop-Ruano,‡ Luis Cerdán,‡ Alejandro Manjavacas,*,‡ and Agustín Mihi*,†

†*Institute of Materials Science of Barcelona (ICMAB-CSIC), Campus de la UAB, 08193, Bellaterra, Spain.*

‡*Instituto de Química Física Blas Cabrera (IQF-CSIC), 28006, Madrid, Spain*

E-mail: a.manjavacas@csic.es; amihi@icmab.es

S1. Geometric parameters of master molds

Lattice parameter, Λ (nm)	Hole diameter, d (nm)	Hole height, h (nm)
300	150	150
400	296	350
500	298	350
600	330	350
Random (correlation distance 500)	300	350

S2. Coverage of the Rhodamine B-doped SU-8 layer

To verify that the layer of Rhodamine B-doped SU-8 conforms to our structures, we inspected the samples using AFM and SEM. Initially, we analyzed a sample with $\Lambda = 400$ nm to measure the depth of the features and confirm that it matches the expected values from the measurements in the master. Figure S1 shows that the depth of the holes in the system without the gain layer was approximately 230 nm after TiO_2 deposition. This measurement is significantly lower than the expected values based on our masters. To investigate further, we examined the sample using SEM to obtain cross-sectional views, as the AFM tip may not be able to penetrate deeply enough to capture the full depth of the holes. Figure S2a presents a SEM cross-sectional image of a sample with the gain layer. Upon measuring the depth of the holes in this image, we obtained a value very close to the 350 nm expected from our master.

Following the deposition of the Rhodamine B-doped SU-8 layer, the holes were filled and no relief was observed on the top surface in the AFM measurements. Therefore, we reassessed the thickness using the SEM micrograph (Fig. S2b), where we measured a value of approximately 270 nm above the top layer of TiO_2, thus confirming that the holes were filled with this layer.

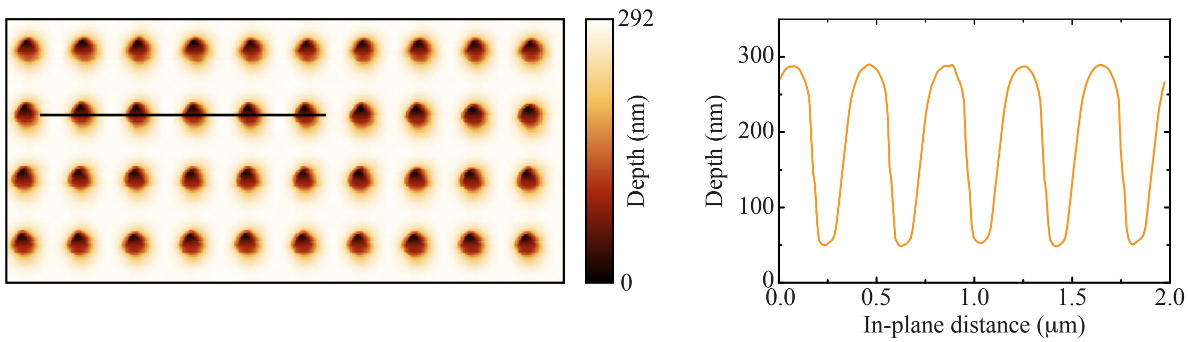

Figure S1: AFM image of a sample with $\Lambda = 400\,\text{nm}$ (left) alongside the profile of the holes corresponding to the line drawn in the image (right).

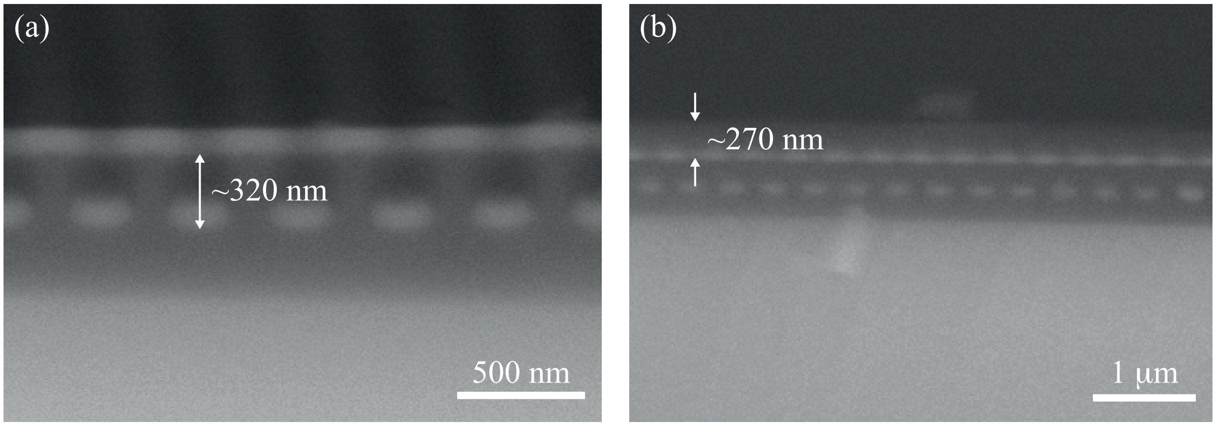

Figure S2: SEM cross-sectional images of a sample after coating it with the gain layer.

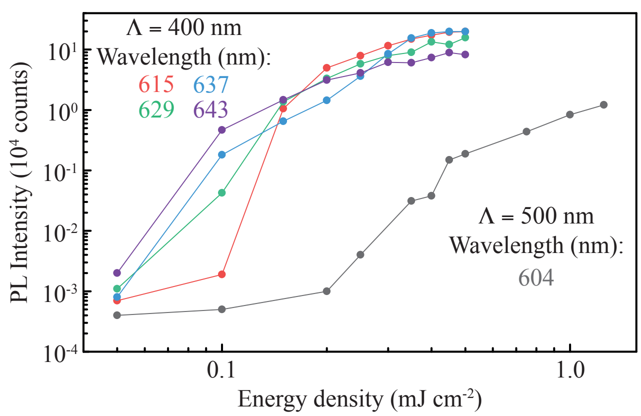

Figure S3: PL intensity at each mode peak wavelength as a function of the excitation energy density. Red, green, blue, and purple dots correspond to the four different peaks of the $\Lambda = 400\,\mathrm{nm}$ array, while the grey dots indicate the results for the system with $\Lambda = 500\,\mathrm{nm}$. Please note that the PL measurements for the system with $\Lambda = 500\,\mathrm{nm}$ were conducted seven months after fabrication, with the sample stored under ambient conditions. This demonstrates the good chemical and structural stability of the samples and materials.

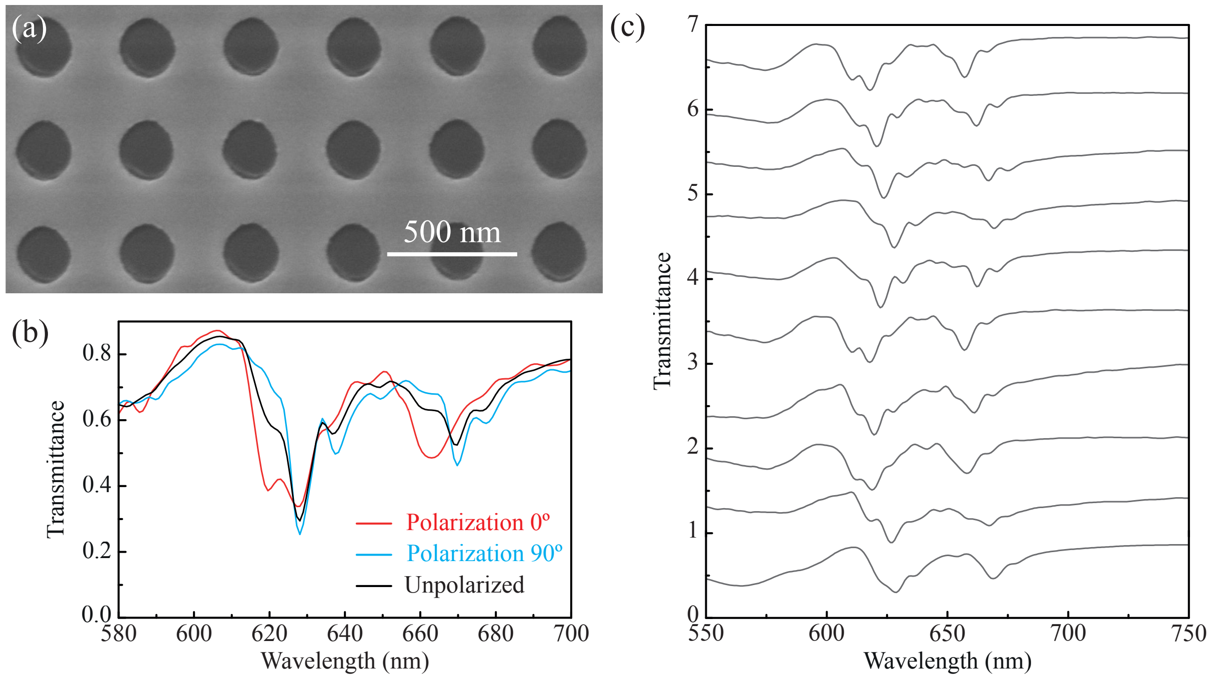

Figure S4: (a) SEM micrograph showing the asymmetric deposition of TiO_2 inside the holes of the array with $\Lambda = 400\,\text{nm}$. (b) Transmittance measured at normal incidence using light with different polarization characteristics. (c) Change in the transmittance spectrum when scanning the illumination spot across the system.

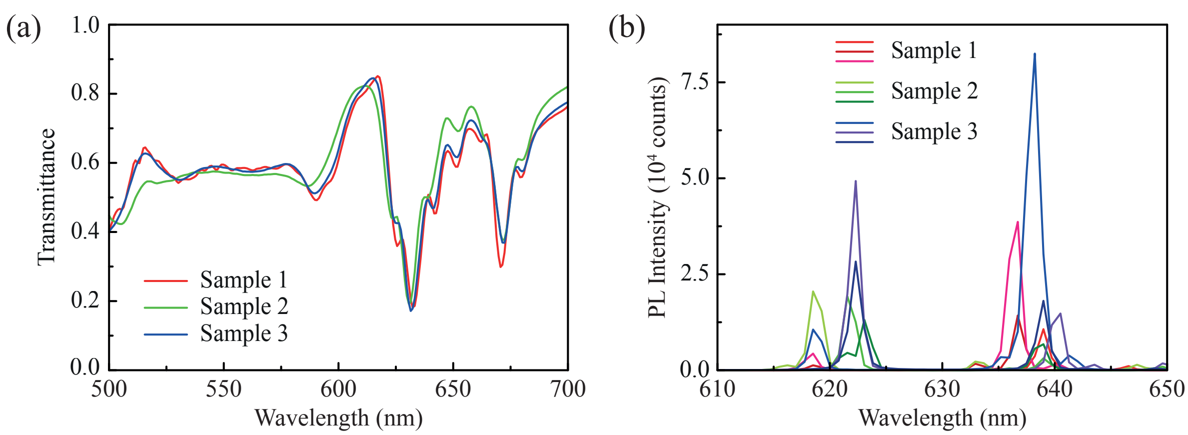

Figure S5: (a) Transmittance for three different samples of arrays with $\Lambda = 400\,\text{nm}$ measured at normal incidence. (b) PL spectra for the three samples of panel (a), measured at three different spots on each sample.

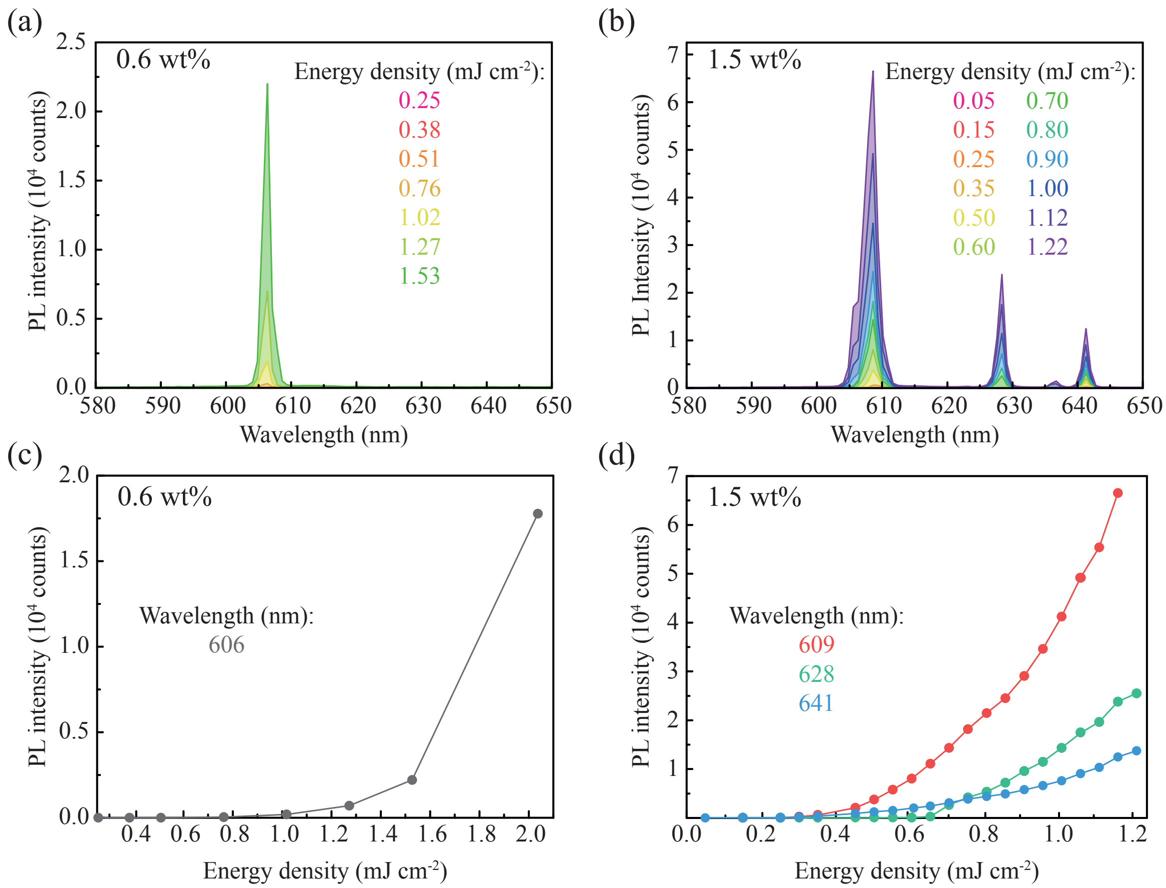

Figure S6: (a,b) PL spectra for the $\Lambda = 400\,\mathrm{nm}$ array with a layer of Rhodamine B-doped SU-8 at dye concentrations of 0.6 wt% (a) and 1.5 wt% (b), measured for increasing excitation energy densities. (c,d) PL intensity at each mode peak wavelength as a function of the energy density, showing the lasing threshold for the samples in (a,b).

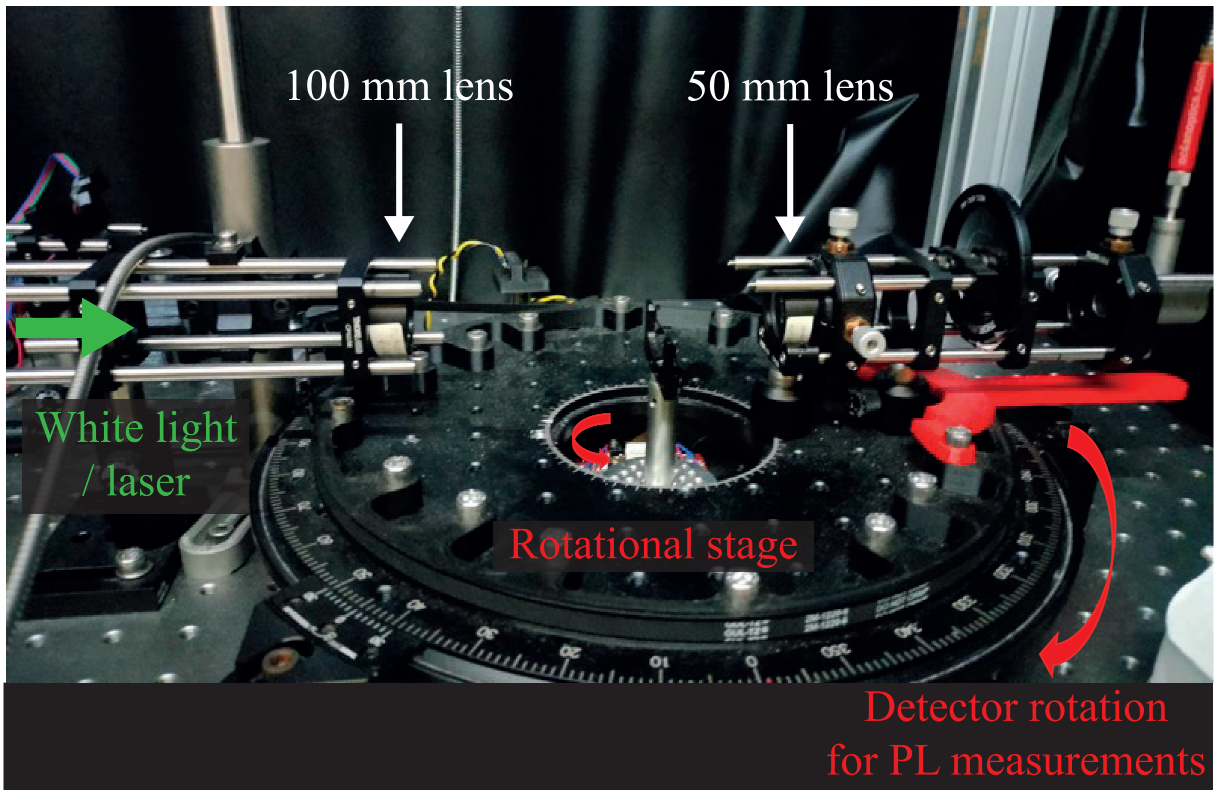

Figure S7: Photograph of the setup used for the angular-resolved transmittance and PL measurements. The sample is mounted on a rotatory stage adjusted to measure the transmittance. The position of the detector can also be adjusted, allowing for the measurement of the angle-resolved PL and the divergence of the lasing emission.